J. Chem. Sci., Vol. 120, No. 1, January 2008, pp. 15–23.

Ultrafast fluorescence resonance energy transfer in a bile salt aggregate: Excitation wavelength dependence

UJJWAL MANDAL, SUBHADIP GHOSH, DIBYENDU KUMAR DAS, ANIRUDDHA ADHIKARI, SHANTANU DEY and KANKAN BHATTACHARYYA*

Physical Chemistry Department, Indian Association for the Cultivation of Science, Jadavpur, Kolkata 700 032

e-mail: pckb@mahendra.iacs.res.in

Abstract. Fluorescence resonance energy transfer (FRET) from Coumarin 153 (C153) to Rhodamine 6G (R6G) in a secondary aggregate of a bile salt (sodium deoxycholate, NaDC) is studied by femtosecond up-conversion. The emission spectrum of C153 in NaDC is analysed in terms of two spectra–one with emission maximum at 480 nm which corresponds to a non-polar and hydrophobic site and another with maximum at ~530 nm which arises from a polar hydrophilic site. The time constants of FRET were obtained from the rise time of the emission of the acceptor (R6G). In the NaDC aggregate, FRET occurs in multiple time scales - 4 ps and 3700 ps. The 4 ps component is assigned to FRET from a donor (D) to an acceptor (A) held at a close distance (R_{DA} ~ 17 Å) inside the bile salt aggregate. The 3700 ps component corresponds to a donor–acceptor distance ~48 Å. The long (3700 ps) component may involve diffusion of the donor. With increase in the excitation wavelength (λ_{ex}) from 375 to 435 nm, the relative contribution of the ultrafast component of FRET (~4 ps) increases from 3 to 40% with a concomitant decrease in the contribution of the ultraslow component (~3700 ps) from 97 to 60%. The λ_{ex} dependence is attributed to the presence of donors at different locations. At a long λ_{ex} (435 nm) donors in the highly polar peripheral region are excited. A short λ_{ex} (375 nm) 'selects' donor at a hydrophobic location.

Keywords. Bile salt; excitation wavelength dependence; femtosecond; FRET.

1. Introduction

Bile salts are biologically important natural surfactant molecules and play an important role in biliary secretion and solubilization of cholesterol, lipid, bilirubin, fat-soluble vitamins and many other species in living organisms.[1] The bile salt, sodium deoxycholate consists of a convex hydrophobic surface (the steroid ring) and a concave hydrophilic surface (hydroxyl groups and carboxylate ions). In a slightly alkaline medium (pH > 7.5), NaDC displays two critical micellar concentrations (CMC_1 and CMC_2) at 10 and 60 mM, respectively. At a lower concentration (~10 mM) bile salt forms a primary aggregate with the polar face (hydroxyl group and ions) pointing outwards (scheme 2a).[1a] At a sufficiently higher concentration (> 60 mM), the secondary aggregates are formed.[1,2] According to small angle neutron scattering (SANS) studies, the secondary aggregate is a long (~40 Å) cylinder with a central water filled tunnel with radius ~8 Å (scheme 2b).[2] The microenvironment and binding dynamics of many fluorescent probes in different sites of a bile salt aggregate has been studied extensively.[3,4]

In the present work, we report on fluorescence resonance energy transfer (FRET) between a donor (coumarin 153, C153) and an acceptor (rhodamine 6G, R6G) inside the secondary aggregate of NaDC. According to the Forster model, the rate of FRET is inversely proportional to the sixth power of distance (R_{DA}) between the donor (D) and the acceptor (A).[5,6] As a result, FRET between a donor and an acceptor held at close proximity in a nanocavity occurs in ultrafast time scale (~ a few ps). The main interest on FRET in confined environment stems from their important role in many biological processes.[5] Most recent applications of FRET include single molecule studies in protein folding,[5b,c] in polymers,[5e] and in nanoparticles.[5f]

Most biological systems are heterogeneous on molecular length scale. In such a system, the donor or the acceptor may reside in drastically different environments.[6,7] The absorption and emission spectra of the donor (C153) depends strongly on the polarity[9] and thus, varies markedly with different

*For correspondence

locations. Both the donor (C153) and the acceptor (R6G) bind strongly to the NaDC aggregate. In the case of the cationic acceptor (R6G), binding to the anionic NaDC aggregate originates mainly from electrostatic and also from hydrophobic interaction. The neutral donor (C153) is sparingly soluble in water and much more soluble in non-polar media. Binding of C153 to NaDC is mainly governed by hydrophobic interactions.

In order to explore FRET in different regions of the bile salt aggregate, we made use of the excitation wavelength (λ_{ex}) dependence of the spectra of the donor (C153). Excitation at a shorter wavelength ('blue edge') selects the donor (C153) residing in a relatively non-polar ('buried') environment and gives rise to a blue shifted emission spectrum. On the contrary, excitation at a longer wavelength ('red edge') selects the probe in a relatively polar ('exposed') site and gives rise to a red shifted emission spectrum. This phenomenon of red shift of emission maximum with increase in λ_{ex}, is known as the red edge excitation shift (REES).[6–8] Excitation wavelength (λ_{ex}) dependence of FRET is relatively less explored. Very recently, we have demonstrated this for a micelle,[6a] gel[6a] and reverse micelle.[6b] In this work, we show that FRET in the interior of a secondary aggregation of bile salt, NaDC exhibits marked dependence on excitation wavelength (λ_{ex}).

2. Experimental

Laser grade coumarin 153 (C153, scheme 1a) and Rhodamine 6G (R6G, scheme 1b) were purchased from Exciton. Bile salt, sodium deoxycholate (NaDC scheme 2) was purchased form Aldrich and used without further purification. In this experiment we used an aqueous solution of NaDC of concentration 105 mM. Donor (C153) and acceptor (R6G) concentrations were kept fixed at 40 μM. The steady state absorption and emission spectra were recorded in a Shimadzu UV-2401 spectrophotometer and a Spex FluoroMax-3 spectrofluorimeter, respectively.

In our femtosecond upconversion set up (FOG 100, CDP), the sample was excited at 375, 405 and 435 nm. Briefly, the sample was excited using the second harmonic of a mode-locked Ti-sapphire laser (Tsunami, Spectra Physics) pumped by a 5 W Millennia (Spectra Physics). The fundamental beam was frequency doubled in a non-linear crystal (1 mm BBO, $\theta = 25°$, $\phi = 90°$). The fluorescence emitted from the sample was upconverted in a non-linear crystal (0·5 mm BBO, $\theta = 38°$, $\phi = 90°$) using a gate pulse of the fundamental beam. The upconverted light is dispersed in a monochromator and detected using photon counting electronics. A cross-correlation function obtained using the Raman scattering from ethanol displayed a full width at half maximum (FWHM) of 350 fs. The femtosecond fluorescence

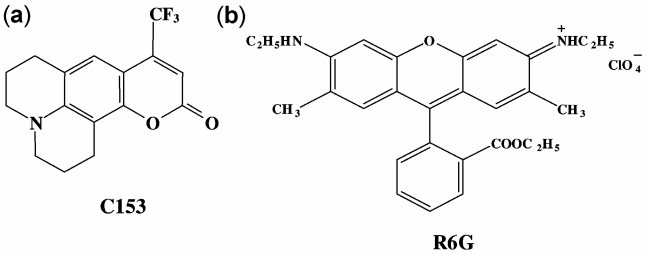

Scheme 1. Schematic representation of Coumarin 153 (**a**) and Rhodamine 6G (**b**).

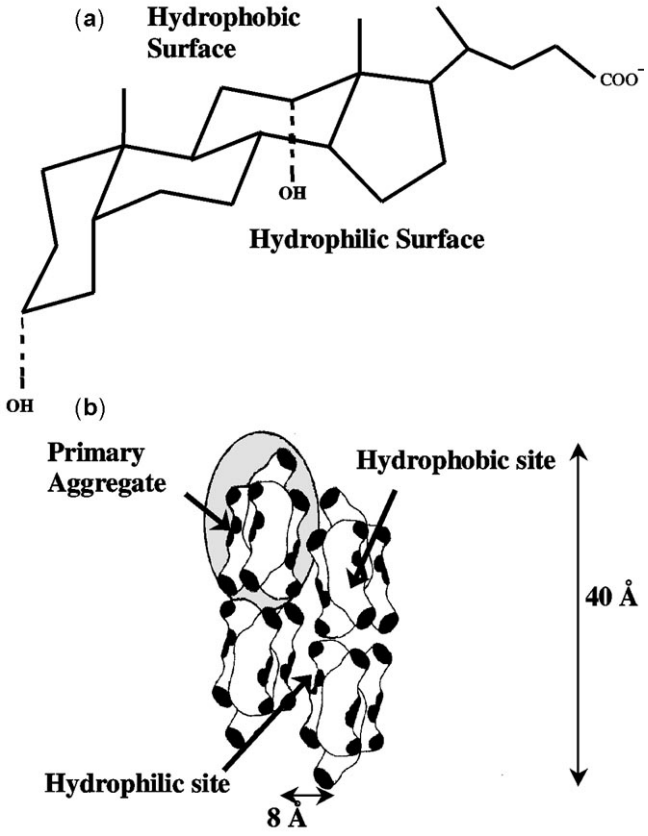

Scheme 2. Schematic representation of (**a**) Bile salt, NaDC, (**b**) Secondary aggregate of NaDC.

decays were fitted using a Gaussian shape for the excitation pulse.

To fit the femtosecond data we used the long picosecond components and kept them fixed during fitting of femtosecond data. The picosecond components were detected using a set up in which the samples were excited at 375, 405 and 435 nm using picosecond diode laser (IBH Nanoleds) in an IBH Fluorocube apparatus. The emission was collected at a magic angle polarization using a Hamamatsu MCP photomultiplier (5000U-09). The time correlated single photon counting (TCSPC) set up consists of an Ortec 9327 CFD and a Tennelec TC 863 TAC. The data is collected with a PCA3 card (Oxford) as a multi-channel analyzer. The typical FWHM of the system response using a liquid scatterer is about 90 ps. The fluorescence decays were deconvoluted using IBH DAS6 software.

In order to study fluorescence anisotropy decay, the analyzer was rotated at regular intervals to get the parallel ($I_{||}$) and perpendicular ($I_{\perp}$) decays. The anisotropy function, $r(t)$ was calculated using the formula

$$r(t) = \frac{I_{||}(t) - GI_{\perp}(t)}{I_{||}(t) + 2GI_{\perp}(t)} \tag{1}$$

The G value of our set up was determined using a probe whose rotational relaxation is very fast, e.g. C153 in methanol and was found to be 1·45.

According to the Förster theory, the rate of FRET, k_{FRET} is given by[5a,b,8a,10]

$$k_{\text{FRET}} = \frac{1}{\tau_D^0}\left(\frac{R_0}{R_{DA}}\right)^6, \tag{2}$$

where, τ_D^0 is the lifetime of the donor in the absence of acceptor. At a donor–acceptor distance $R_{DA} = R_0$, the efficiency of energy transfer is 50% and $k_{FRET} = (1/\tau_D)$. The Förster distance R_0 (in Å) is given by,[5a,b,6,8a,10]

$$R_0 = 0.211[\kappa^2 n^{-4} Q_D J(\lambda)]^{1/6}, \tag{3}$$

where, Q_D is the quantum yield of the donor in the absence of acceptor, n is the refractive index of the medium (~1·4 for macromolecules in water),[10] κ^2 is the orientation factor and $J(\lambda)$ is the spectral overlap between the donor emission and the acceptor absorption. $J(\lambda)$ is related to the normalized fluorescence intensity (F_D) of the donor in the absence of the acceptor and the extinction coefficient of the acceptor (ε_A) as,[6,8a,10]

$$J(\lambda) = \frac{\int_0^\infty F_D(\lambda)\varepsilon_A(\lambda)\lambda^4 \mathrm{d}\lambda}{\int_0^\infty F_D(\lambda)\mathrm{d}\lambda} \tag{4}$$

The value of κ^2 may vary from 0 (mutually perpendicular transition dipoles) to 4 (collinear dipoles). For $\kappa^2 = 0$, FRET is forbidden and no ultrafast component of FRET would be observed. The ultrafast FRET detected in this work obviously indicates a large value of κ^2. One can estimate the upper ($\kappa^2_{\max}$) and lower ($\kappa^2_{\min}$) limit of κ^2 following the recipe prescribed by Lakowicz and co-workers.[10] The values of $\kappa^2_{\max}$ and $\kappa^2_{\min}$ are given by[10]

$$\kappa^2_{\min} = \frac{2}{3}\left[1 - \frac{(d_D^x + d_A^x)}{2}\right] \tag{5}$$

$$\kappa^2_{\max} = \frac{2}{3}(1 + d_D^x + d_A^x + 3d_D^x d_A^x) \tag{6}$$

where, d_i^x denotes the ratio of square root of the steady state fluorescence anisotropy (r_i^{SS}) and the initial value of anisotropy (r_i^0) in the anisotropy decay of the ith species (donor or acceptor). However, the distance calculated using Förster model may vary by only about ≤ 20% in the range of values of κ^2.[6b,8a] We therefore used $\kappa^2 = 2/3$ (random orientation) for the calculation of R_0.

In order to decompose the steady state emission spectrum into multiple spectra, we have assumed a log-normal spectral function e.g.

$$I(\lambda) = I_0 \exp\{-\ln 2[\ln\{1 + 2b(\lambda - \lambda_p)/w\}/b]^2\}, \tag{7}$$

where, I_0 is peak height, λ_p is the emission maximum, b is the asymmetric factor, w denotes width of the spectrum.

3. Results and discussions

3.1 *Steady state absorption and emission spectra: λ_{ex} dependence*

In pure water, C153 exhibits an absorption peak at 430 nm and an emission peak at ~549 nm (figure

1a). Solubility of C153 increases markedly on addition of NaDC. The absorption and emission spectra of C153 in 105 mM NaDC, are markedly blue shifted compared to those in water. In 105 mM NaDC solution, the absorption maximum of C153 is at 424 nm and is blue shifted by ~6 nm from the reported[9] absorption maximum of C153 in water. The emission spectrum of C153 in NaDC is found to be much broader than that in water and shows a peak at

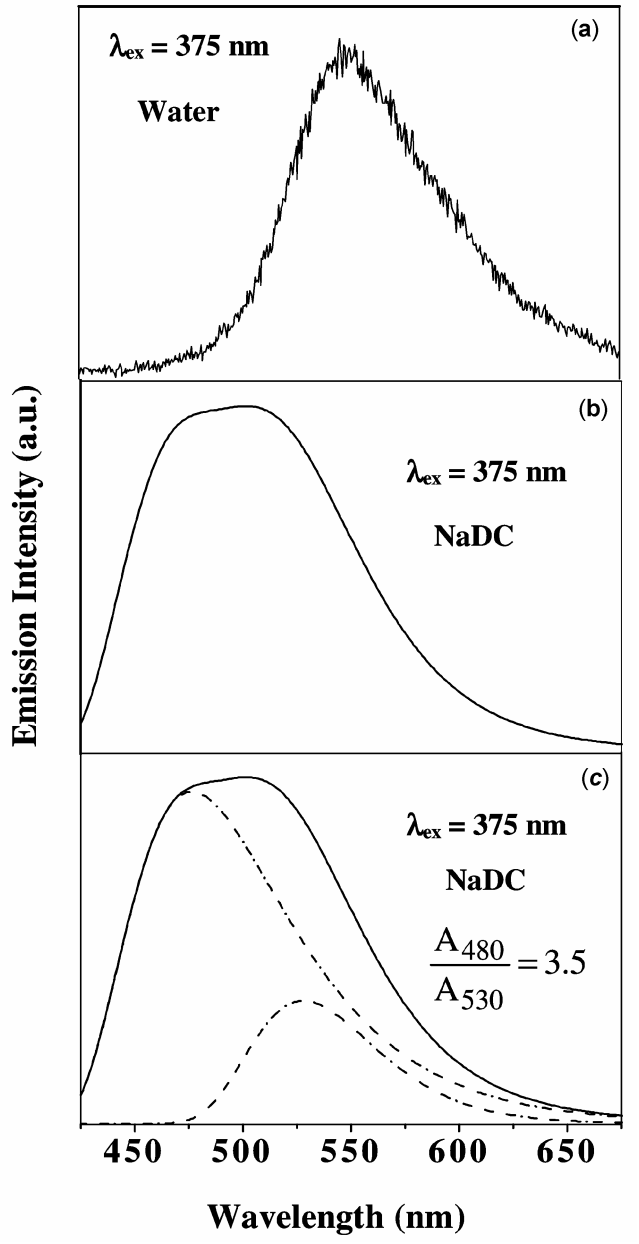

Figure 1. Emission spectra of C153 in (**a**) water (λ_{ex} = 375–435 nm), (**b**, **c**) NaDC (105 mM, λ_{ex} = 375 nm, solid line). (**c**) Splitted spectrum (dotted line) of C153 in NaDC (λ_{ex} = 375 nm) for the buried and exposed region. Ratio of the areas of emission spectra in polar region to that in non-polar is indicated (A denotes area under curve with emission maxima mentioned as subscript).

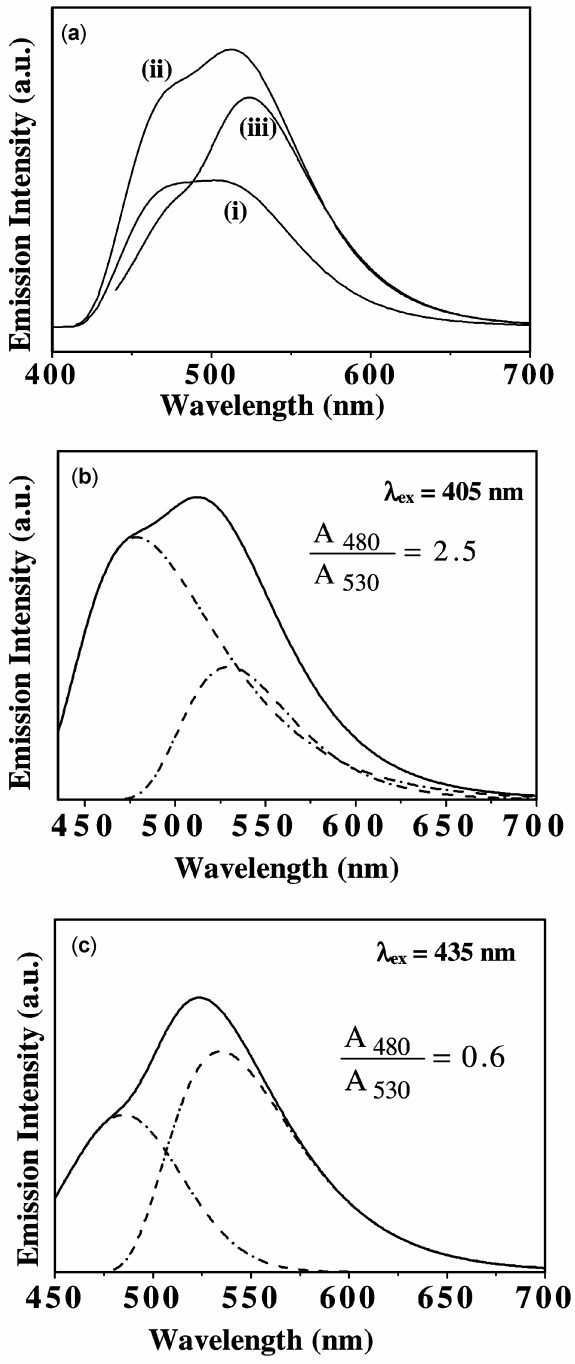

Figure 2. Emission spectra of C153 in 105 mM NaDC at (**a**) λ_{ex} = 375 nm (i), 405 nm (ii) and 435 nm (iii). (**b**, **c**) Splitted spectrum of C153 in 105 mM NaDC (dotted line) at λ_{ex} = 405 nm (**b**) and 435 nm (**c**), solid lines show the experimental spectra. Ratios of the areas of emission spectra in polar region to that in non-polar are indicated (A denotes area under curve with emission maxima mentioned as subscript).

~520 nm and a prominent shoulder at ~480 nm (figure 1b, 2a). With increase in λ_{ex} from 375 to 435 nm, the shape of the emission spectrum of C153 in NaDC changes markedly and displays a sharp decrease in the intensity of the shoulder region (figure 2a). The broadness of the emission spectrum and the λ_{ex} dependence suggest presence of multiple locations of C153 inside the NaDC aggregate. The emission spectrum of C153 in NaDC may be resolved as a superposition of two spectra one with maximum at 480 nm and another with maximum ~530 nm (figures 1c and 2b–c). In summary, in the NaDC aggregate C153 molecules are distributed in two locations with distinctly different emission maximum (480 and 530 nm). From the reported emission maxima of C153 in different solvents[9] the 480 nm emission peak corresponds to a relatively non-polar hydrophobic location whose polarity is intermediate between cyclohexane and ethyl acetate. The 530 nm emission peak of C153 may arise from a polar and hydrophilic region which is similar to ethanol. The relative intensity (area) of the two emission spectra (A_{480}/A_{530}) decreases from 3·5 at λ_{ex} = 375 nm to 0.6 at λ_{ex} = 435 nm. It is obvious that with increase in λ_{ex} contribution of the polar (exposed) region (maximum at 530 nm) increases with a concomitant decrease in the contribution of the non-polar (buried) region (peak at 480 nm).

The absorption maximum of rhodamine 6G (R6G) in NaDC is observed to be at 537 nm. This is red shifted by 11 nm from that of R6G in water.[8a] The emission maximum (567 nm) of R6G in bile salt aggregate is found to be red shifted from that (550 nm) in water. The emission maximum of R6G in 105 mM does not display any λ_{ex} dependence. This indicates that the cationic dye (R6G) is predominantly localized in the polar and exposed site of NaDC.

3.2 *λ_{ex} dependence of spectral overlap and FRET from C153 to R6G*

Addition of the acceptor (R6G) to a solution of C153 in 105 mM NaDC causes a marked decrease in the emission intensity of the donor (figure 3) because of FRET from C153 to R6G. Interestingly, as shown in figure 3, the extent of quenching of the donor emission depends on λ_{ex}. It is observed that the extent of quenching of donor emission (i.e. FRET) is maximum for a long λ_{ex} (435 nm, figure 3c) and minimum for a short λ_{ex} (375 nm, figure 3a). This may be explained as follows. As noted earlier, the donor (C153) is distributed over the polar and non-polar site while the R6G is preferentially local-

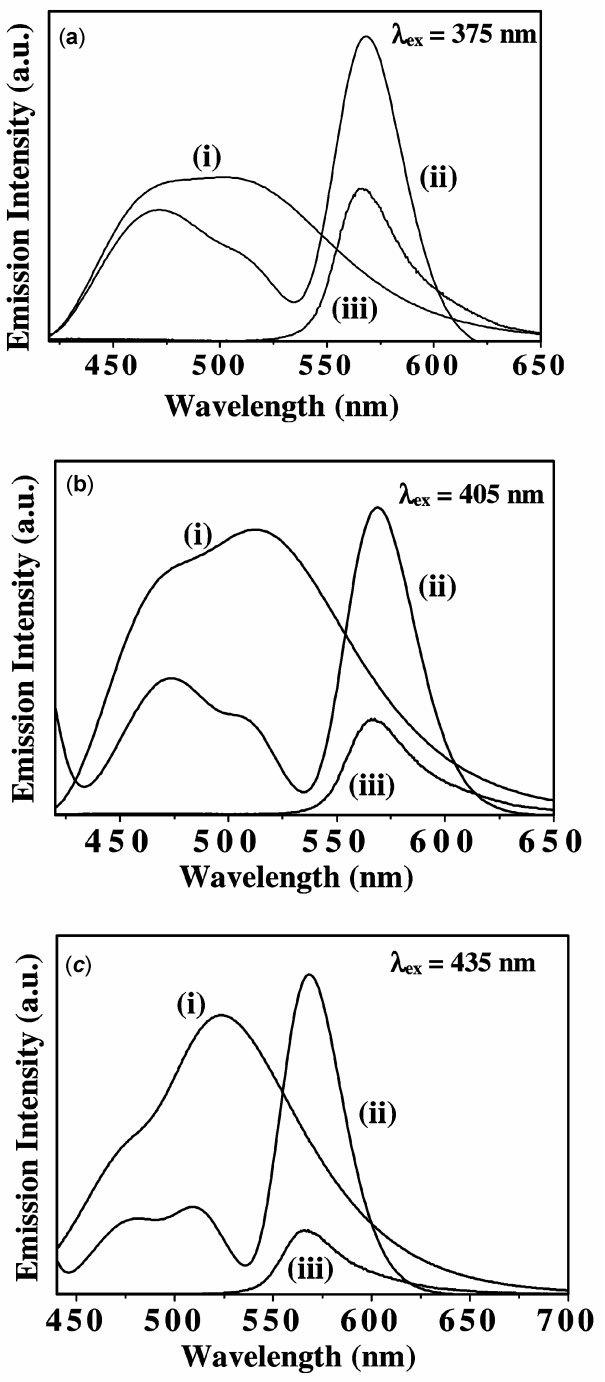

Figure 3. Emission spectra of C153 (40 μM) in 105 mM NaDC in the absence (i) and presence (ii) of 40 μM R6G at λ_{ex} = 375 (**a**), 405 (**b**) and 435 nm (**c**); while (iii) in each case denotes the emission spectrum of R6G (40 μM) in 105 mM NaDC.

Table 1. Energy transfer parameters for C153-R6G pair in 105 mM NaDC.

$J(\lambda)$* ($M^{-1}cm^{-1}nm^4$)		R_0 (Å)		Steady state efficiency of FRET (ε_s*)	
Peak 1 (buried)	Peak 2 (exposed)	Peak 1 (buried)	Peak 2 (exposed)	Peak 1	Peak 2
$1{\cdot}9 \times 10^{15}$	$3{\cdot}9 \times 10^{15}$	50 ± 1	56 ± 1	0·15	0·60

*± 10%

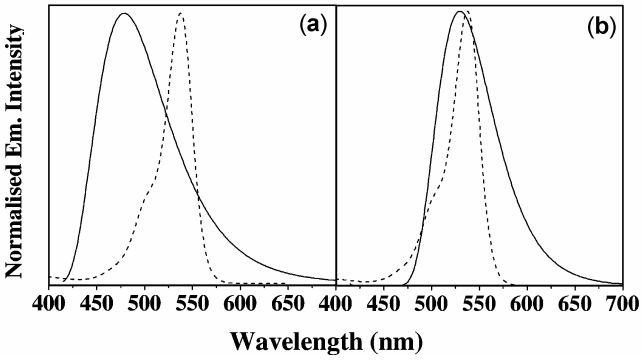

Figure 4. Spectral overlap of donor (C153) emission (solid line) with acceptor R6g absorption (dotted line) in 105 mM NaDC for the buried (**a**) and the exposed (**b**) region (donor emission obtained from the spectral splitting).

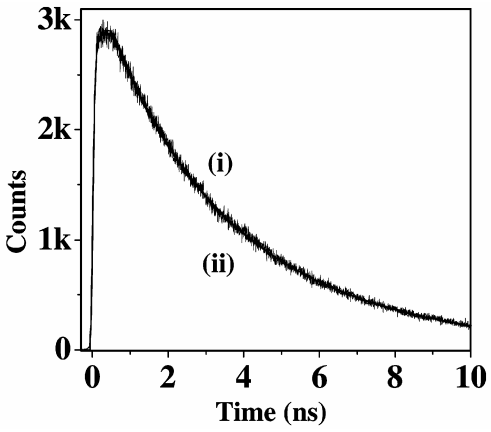

Figure 5. Picosecond fluorescence transient (λ_{em} = 465 nm) of 40 μM C153 (donor) in 105 mM NaDC in the absence (i) and in the presence (ii) of 40 μM R6G (λ_{ex} = 405 nm).

ized in the polar site. A long λ_{ex} (435 nm) selects the polar site where the donor and the acceptor are close to each other and hence, displays very efficient FRET. For a short λ_{ex} (375 nm) donors in the non-polar region are excited which are far from the acceptor and hence, efficiency of FRET diminishes.

Table 2. Femtosecond decay parameters of R6G (40 μM, λ_{em} = 570 nm) in the absence of C153 at different λ_{ex}.

Medium	λ_{ex} (nm)	τ_1* (a_1) (ps)	τ_2* (a_2) (ps)
NaDC (105 mM)	375	–	6900 (1·00)
	405	–	6500 (1·00)
	435	100 (0·13)	6800 (0·87)

*± 10%

In order to understand the λ_{ex} dependence of FRET we studied the spectral overlap of the acceptor absorption with the donor emission for the buried and the exposed regions. Figure 4 shows the spectral overlap in these two cases. The efficiency (ε_s) of FRET was calculated from the steady state emission intensities. If I_{DA} and I_D, denote the emission intensity of the donor in the presence and absence of the acceptor, the efficiency of FRET is given by, $\varepsilon_s = 1 - (I_{DA}/I_D)$.[8a,10]

The efficiency of FRET (ε_s), overlap integral ($J(\lambda)$) and the Forster distance (R_0) for the two sites of the donor at different λ_{ex} are summarized in table 1. It is readily seen that the efficiency of FRET for the buried region (donor emission maximum ~480 nm) is much lower than that for the exposed region (donor emission maximum ~530 nm). For instance, at λ_{ex} = 375 nm the efficiency for the buried region (0·15) is about 4 times smaller than that (0·6) for the exposed site. With increase in λ_{ex}, the relative contribution of the exposed site increases (figures 1 and 2) and this causes an increase in the efficiency of FRET.

3.3 *Time resolved studies of FRET from C153 to R6G in bile salt aggregate*

3.3a *Picosecond studies of donor decay:* FRET is commonly monitored by shortening of the donor life time.[10] Figure 5 shows picosecond fluorescence decays of the donor (C153) at 465 nm in 105 mM NaDC in the absence and presence of acceptor

Table 3. Excitation wavelength (λ_{ex}) dependence of rise of acceptor (40 μM R6G) in the presence of 40 μM donor (C153) in 105 mM NaDC at λ_{em} = 570 nm.

λ_{ex} (nm)	τ_1* (a_1) (ps)	τ_2* (a_2) (ps)	τ_3* (a_3) (ps)
375	4 (–0·10, 3%)	3700 (–3·06, 97%)	7000 (4·16)
405	4 (–0·12, 13%)	3700 (–0·83, 87%)	7000 (1·95)
435	4 (–0·13, 40%)	3700 (–0·20, 60%)	7000 (1·33)

* ± 10%

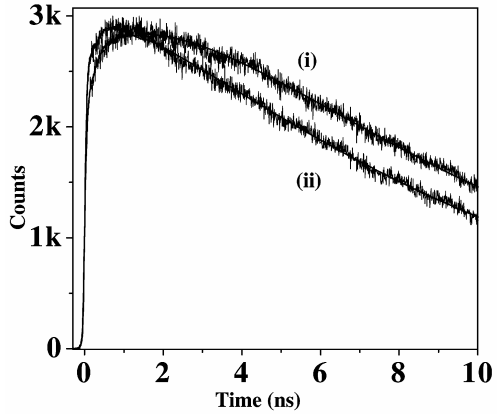

Figure 6. Picosecond fluorescence decays of acceptor R6G (at λ_{em} = 570 nm) in 105 mM NaDC in the presence of donor (C153) for (i) λ_{ex} = 375 nm and (ii) λ_{ex} = 435 nm.

(R6G) at λ_{ex} = 405 nm. It is readily seen that in 105 mM NaDC, addition of the acceptor (R6G) does not affect the average decay time of C153. This result which is in apparent contradiction with steady state emission intensities may be explained as follows. The fluorescence decay is dominated by the unquenched (non-FRET) donors in a bile salt aggregate with no acceptor.[6,8a,12] The life time of the donor molecules which have an acceptor in the immediate vicinity in the same micelle is often too short to measure using a picosecond set up. Thus, the picosecond study of the donor lifetime incompletely describes FRET from C153 to R6G in NaDC.

3.3b *Picosecond studies of acceptor fluorescence:* In order to determine the ultrafast components of FRET we studied the rise time of the acceptor (R6G) emission.[6,8a] According to Tachiya[13a,b] the rise of the acceptor emission is given by $-\exp[-n(1-\exp(-k_{FRET}\,qt)]$ where n is the average number of acceptor per micelle. For times shorter than $1/k_{FRET} < 1$, the initial ultrafast rise is given by $-\exp(-k_{FRET}t)$ (since in this case $n \sim 1$).

The fluorescence transients of the acceptor (R6G) were studied at an emission wavelength (λ_{em})

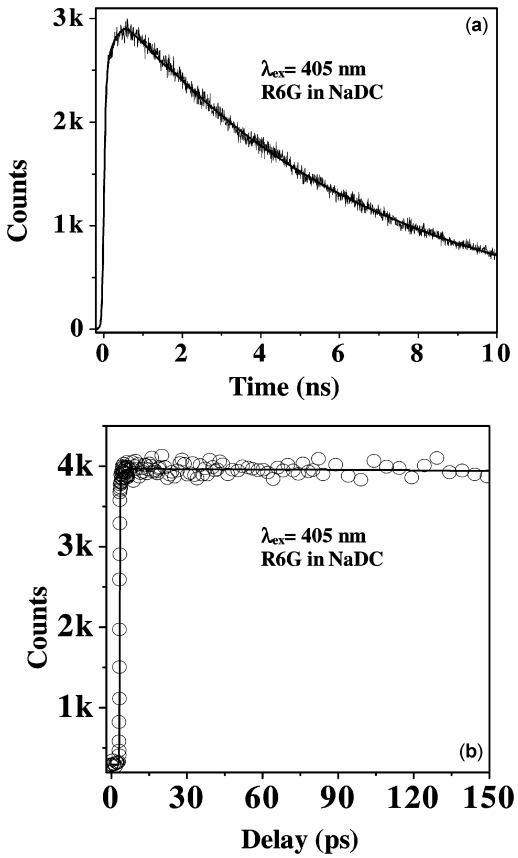

Figure 7. Picosecond (**a**) and femtosecond (**b**) fluorescence transient (λ_{em} = 570 nm) of 40 μM R6G in 105 mM NaDC in the absence of C153 (donor) (λ_{ex} = 405 nm).

570 nm where the contribution of the quenched donor emission is negligible. In 105 mM NaDC, acceptor (R6G) shows a single exponential decay (λ_{em} = 570 nm) with no rise components in the absence of the donor (C153) (figure 6, table 2). In the presence of the donor, in NaDC, the picosecond transient of the acceptor (R6G) at 570 nm shows a rise time of 3700 ps (figure 6 and table 3).

3.3c *Femtosecond study of the acceptor transients:* For the detection of the ultrafast components of FRET, we used a femtosecond up-conversion set up. In the absence of the donor no rise component is observed in the acceptor emission (figure 7, table 2).

Using the femtosecond set up, we detected both ultrafast rise time of the acceptor emission (figure 8) and an ultrafast decay component of the donor emission in the presence of the acceptor. Shortening of donor life time and the appearance of growth in acceptor's decay unambiguously confirms ultrafast FRET from donor (C153) to an acceptor (R6G) in NaDC.

Figure 8 shows the femtosecond rise of the acceptor (R6G) in the presence of donor (C153) at an emission wavelength of 570 nm in 105 mM NaDC solution at different λ_{ex}. For all λ_{ex}, we have detected an ultrafast (4 ps) rise component of the acceptor emission (i.e. of FRET) in addition to 3700 ps component (table 3). As shown in table 3, the relative contribution of the ultrafast rise component increases markedly with increase in λ_{ex}. With increase in excitation wavelength from 375 to 435 nm, contribution of the 3700 ps rise time decreases from 97 to 60%, respectively (table 3).

3.4 *Donor–acceptor distances: λ_{ex} dependence of FRET*

The donor–acceptor distances (R_{DA}) corresponding to the FRET components (= $1/k_{FRET}$) 4 ps and 3700 ps were determined using equation (2) and the calculated values of R_0. The 4 ps component corresponds to R_{DA} = 17 Å which is close to the sum of the radii of the donor and the acceptor. The ionic acceptor resides preferentially in the polar region. Thus the 4 ps component of FRET arises from FRET between the donor and the acceptor, both in the polar region. Obviously, with increase in λ_{ex}, contribution of the donors in the polar region increases. As a result, with increase in λ_{ex}, contribution of the 4 ps component increases from 3% at λ_{ex} = 375 nm to 40% at λ_{ex} = 435 nm (table 3).

The 3700 ps component of FRET corresponds to R_{DA} = 48 Å. Thus it arises from donor which are residing in the non-polar region far from the ionic acceptor. With increase in λ_{ex}, contribution of the non-polar region decreases and hence, contribution of the 3700 ps component decreases from 97% at λ_{ex} = 375 nm to 60% at λ_{ex} = 435 nm (table 3).

The donor molecules diffuse over a distance $(2D_t\tau_{FRET})^{1/2}$ in the timescale of FRET (τ_{FRET}). For organic molecules in a micelle the translational diffusion D_t is of the order 0·5–50 Å^2/ns.[14–16] For 105 mM NaDC aggregate the ultrafast component of FRET: 4 ps and the long 3700 ps component correspond to diffusion lengths of 1·3 Å and 38·5 Å, respectively. Obviously, diffusion of donors in the 4 ps time scale of FRET is smaller than molecular dimensions. However, for the 3700 ps component one can not neglect diffusion of donors.

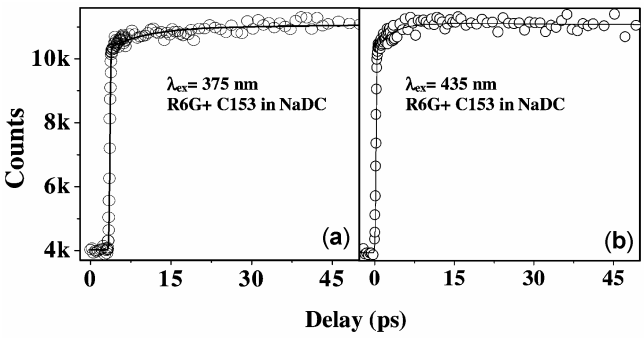

Figure 8. Femtosecond fluorescence transients of R6G (at λ_{em} = 570 nm) in 105 mM NaDC in the presence of donor (C153) for (**a**) λ_{ex} = 375 nm and (**b**) λ_{ex} = 435 nm.

3.5 *Excitation wavelength (λ_{ex}) dependence of anisotropy decay of C153*

In bulk water, the time constant of fluorescence anisotropy decay of C153 is ~100 ps.[11] The fluores-

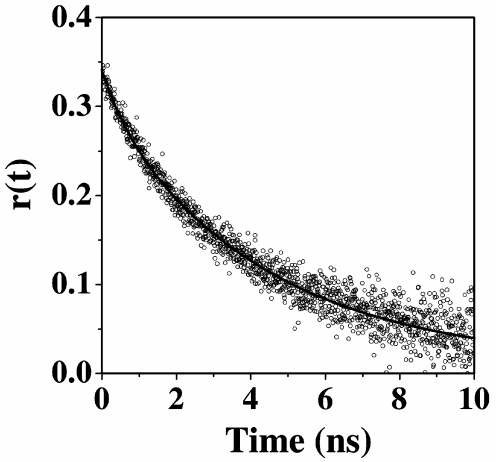

Figure 9. Fluorescence anisotropy decay of C153 in 105 mM NaDC at λ_{ex} = 405 nm (λ_{em} = 465 nm) (O).The points denote the actual values of anisotropy and the solid lines denote the best fit to the experimental data.

Table 4. Parameters of anisotropy decay of C153 in NaDC (105 mM) for λ_{ex} = 405 nm.

λ_{em} (nm)	r_0	τ_{fast} (ps) (a_{fast})	τ_{slow} (ps) (a_{slow})
465	0·34	600 ± 50 (0·13)	4200 ± 200 (0·87)

cence anisotropy decay of C153 in bile salt aggregate (at blue side of the peak, 465 nm, figure 9) is found to be much slower and is fitted to a biexponential function,

$$r(t) = r_0[\beta\exp(-t/\tau_{slow}) + (1 - \beta)\exp(-t/\tau_{fast})]. \quad (8)$$

The high value of initial anisotropy ($r_0 = 0{\cdot}34$) in bile salt aggregate (table 4) suggests that our picosecond set up captures almost the entire rotational dynamics in this case. For $\lambda_{ex} = 405$ nm, the anisotropy decay of C153 in NaDC is described by two decay components of 600 ps (13%) and 4200 ps (87%) (figure 9, table 4). The anisotropy decay of C153 in NaDC does not show appreciable dependence on λ_{ex}.

4. Conclusion

This work demonstrates that the FRET in bile salt aggregate occurs on multiple time scale–4 and 3700 ps. The 4 ps component is assigned to both donor and acceptor residing at close proximity in the polar region ($R_{DA} = 17$ Å). The 3700 ps component arises due to FRET from a donor in the non-polar region to an acceptor in the polar region ($R_{DA} = 48$ Å). It is further shown that with increase in λ_{ex}, contribution of FRET from the donor in the polar region (4 ps component) increases and that due to donor in the non-polar region (3700 ps component) decreases.

Acknowledgements

The authors thank the Department of Science and Technology (DST), (IR/11/CF-01/2002 and J. C. Bose Fellowship) and Council of Scientific and Industrial Research (CSIR) for generous research grants. U M, S G, D K D, A A and S D thank CSIR for awarding fellowships. K B thanks Prof. B Bagchi and M Tachiya for many useful suggestions.

References

1. (a) Small D M 1971 *The bile acid* (Plenum: New York), vol 1, p. 302; (b) O'connor C J and Wallace R G 1985 *Adv. Colloid Interface Sci.* **22** 1; (c) Borgtstorm B, Barrowman J A and Lindstorm M 1985 In *Sterols and bile acid* (eds) H Danielsson and J Sjoval (Amsterdam: Elsevier)
2. (a) Leggio C, Galantini L and Zaccarelli E 2005 *J. Phys. Chem.* **B109** 23857; (b) Hjelm R P, Schteingert C D, Hofman A F and Thiagrajan P 2000 *J. Phys. Chem.* **B104** 197; (c) Santhanlakshmi J, Shantha Lakshmi G, Aswal V K and Goyal P S 2001 *Proc. Indian Acad. Sci., Chem. Sci.* **113** 55; (d) Lopez F, Samseth J, Mortensen K, Rosenqvist E and Rouch J 1996 *Langmuir* **12** 618; (e) Esposito G, Giglio E, Pavel N V and Zanobi A 1987 *J. Phys. Chem.* **91** 356
3. (a) Megyesi M and Biczok L 2007 *J. Phys. Chem.* **B111** 5635; (b) Yihwa C, Quina F H and Bohne C 2004 *Langmuir* **20** 9983; (c) Waissbluth O L, Morales M C and Bohne C 2006 *J. Photochem. Photobiol.* **82** 1030; (d) Gouin S and Zhu X X 1998 *Langmuir*. **14** 4025; (e) Ju C and Bohne C 1996 *J. Phys. Chem.* **100** 3847
4. Sen S, Dutta P, Mukherjee S and Bhattacharyya K 2002 *J. Phys. Chem. B* **106** 7745
5. (a) Wong K F, Bagchi B and Rossky P J 2004 *J. Phys. Chem.* **A108** 5752; (b) Srinivas G and Bagchi B 2001 *J. Phys. Chem.* **B105** 9370; (c) Schuler B, Lipman E A, Steinbach P J, Kumke M and Eaton W A 2005 *Proc. Natl. Acad. Sci. USA* **102** 2754; (d) Kuzmenkina E V, Heyes C D and Nienhaus G U 2005 *Proc. Natl. Acad. Sci. USA* **102** 15471; (e) Cotlet M, Vosch T, Habuchi S, Weil T, Mullen K, Hofkens J and Schryver F De 2005 *J. Am. Chem. Soc.* **127** 9760; (f) Goldman E R, Medintz I L, Whitley J L, Hayhurst A, Clapp A R, Uyeda H T, Deschamps J R, Lassman M E and Mattoussi H 2005 *J. Am. Chem. Soc.* **127** 6744
6. (a) Ghosh S, Dey S, Adhikari A, Mandal U and Bhattacharyya K 2007 *J. Phys. Chem.* **B111** 7085; (b) Mondal S K, Ghosh S, Sahu K, Mandal U and Bhattacharyya K 2006 *J. Chem. Phys* **125** 224710
7. (a) Lakowicz J R 1984 *Biochemistry* **23** 3013; (b) Demchenko A P 1982 *Biophys. Chem.* **15** 101; (c) Mukherjee S and Chattopadhyay A 2005 *Langmuir* **21** 287
8. (a) Sahu K, Ghosh S, Mondal S K, Ghosh B C, Sen P, Roy D and Bhattacharyya K 2006 *J. Chem. Phys.* **125** 044714; (b) Satoh T, Okuno H, Tominaga K and Bhattacharyya K 2004 *Chem. Lett.* **33** 1090; (c) Sen, P, Satoh T, Bhattacharyya K and Tominaga K 2005 *Chem. Phys. Lett.* **411** 339; (d) Sen P, Ghosh S, Mondal S K, Sahu K, Roy D, Bhattacharyya K and Tominaga K 2006 *Chem. Asian. J.* **1** 188
9. Jones II G, Jackson W R, Choi C-Y and Bergmark W R 1985 *J. Phys. Chem.* **89** 294
10. Lakowicz J R 2006 *Principles of fluorescence spectroscopy* (New York: Springer), Chap. 9, 13, 14 and 15, 3rd edn
11. Hazra P, Chakrabarty D, Chakraborty A and Sarkar N 2004 *Biochem. Biophys. Res. Commun.* **314** 543
12. Kenney-Wallace G A, Flint J H and Wallace S C 1975 *Chem. Phys. Lett.* **32** 71
13. (a) Tachiya M 1975 *Chem. Phys. Lett.* **33** 289; (b) Tachiya M 1982 *J. Chem. Phys.* **76** 340
14. Matzinger S, Weidemaier K and Fayer M D 1997 *Chem. Phys. Lett.* **276** 274
15. Quitevis E L, Marcus A H and Fayer M D 1997 *J. Phys. Chem.* **97** 5762
16. Sen P, Ghosh S, Sahu K, Mandal S K, Roy D and Bhattacharyya K 2006 *J. Chem. Phys.* **124** 204905